2,2-Bis[4-(3,4-Dicarboxyphenoxy) Phenyl]Propane Dianhydride (BPADA)-Based Polyimide Membranes for Pervaporation Dehydration of Isopropanol: Characterization and Comparison with 4,4′-(Hexafluoroisopropylidene) Diphthalic Anhydride (6FDA)-Based Polyimide Membranes

Shude Xiao, Xianshe Feng, Robert Y. M. Huang

Department of Chemical Engineering, University of Waterloo, Waterloo, ON, Canada N2L 3G1

Received 14 June 2007; accepted 20 November 2007
DOI 10.1002/app.28734
Published online 9 July 2008 in Wiley InterScience (www.interscience.wiley.com).

ABSTRACT: Polyimides were synthesized from one-step polycondensation of BPADA and various diamines and were characterized with GPC, FTIR, NMR, DSC, and TGA. Polyimide membranes were prepared, and their hydrophilicity was estimated by contact angles and the free energies of interfacial interactions. Pervaporation properties were investigated for the dehydration of isopropanol, and comparisons were made between BPADA-based membranes and 6FDA-based membranes. The concentration coefficients of BPADA-based membranes were calculated from the linear moiety contribution method based on the results from 6FDA-based membranes, and they were compared to understand the effects of the feed concentration on pervaporation properties. The effects of temperature on permeation flux were studied with permeation activation energies for total flux and water flux in permeates. Moiety contribution factors for activation energies were used to correlate permeation flux and monomer moieties in the polymers, and reasonable results were obtained for BPADA. It is revealed that steric effects of monomers may change the diffusion properties, while functional groups are favorable to the changes in sorption properties. © 2008 Wiley Periodicals, Inc. J Appl Polym Sci 110: 283–296, 2008

Key words: polyimide; membrane; pervaporation dehydration; polycondensation; NMR

INTRODUCTION

Mass transport in pervaporation follows the solution-diffusion mechanism. Solubility/sorption and diffusivity properties of the penetrants in the membrane determine the membrane permeability and have to be taken into consideration when selecting a membrane for a particular mixture to be separated. Dehydration of solvents, as the first industrial application of pervaporation, keeps attracting interest from researchers to improve permselectivities of membranes.[1] Because hydrophilic membranes, which are essentially required for pervaporation dehydration, usually undergo severe swelling when they are in contact with the feed, high flux is observed but selectivity is low.[2] Therefore, crosslinking is necessarily needed to achieve the long-term stability.[3] In most cases, crosslinking may cause a decrease in hydrophilicity and cut down the permeability of water, leading to a lower selectivity. Such effects can be simplified if hydrophilic glassy polymers are used as membranes: the hydrophilicity contributes to a good selectivity and the glassy polymer matrices restrict swelling caused by water, though the flux is lower if compared with rubbery polymers. Hence, in this work, polyimides were chosen as membrane materials for pervaporation dehydration of isopropanol.

Known as thermally stable polymers, polyimides have excellent chemical resistance and great mechanical properties,[4] thereby gaining reputation in membrane technologies. Thermal imidization of polyimide precursors, poly(amic acid)s, yields insoluble polyimides, which limited the applications of polyimides in early years.[5] Nevertheless, development of the two-stage polymerization with chemical imidization and the one-step high temperature polymerization offers more opportunities to polyimides as membrane materials.[6]

Some researchers applied commercial polyimide materials to pervaporation dehydration processes. Huang and Feng[7–10] investigated the pervaporation properties of Ultem 1000 (G.E. Plastics, Pittsfield, MA)

Correspondence to: R. Y. Huang (ryhuang@engmail.uwaterloo.ca).

Contract grant sponsor: Natural Sciences and Engineering Research Council (NSERC) of Canada.

in dehydration of ethanol and isopropanol. Yanagishita et al.[11] prepared asymmetric membranes for water/ethanol separation using PI-2080 (Dow Chemical, Midland, MI). Various P84 polyimide (HP Polymer GmbH, Lewisville, TX) membranes were fabricated and successfully used in dehydration of alcohols.[12–14] Guo and Chung[15] studied the thermal hysteresis behaviors in pervaporation dehydration with Matrimid 5218 polyimide (Ciba Polymers, Basel, Switzerland) membranes, and Zhou and Koros[16] used Matrimid hollow fibers to dehydrate acetic acid. In addition, some research focused on the modifications of the commercial polyimides to optimize the dehydration properties of the membranes.[17–19]

On the other hand, molecular design proved to be an efficient way to control the physiochemical properties of the membranes, and attempts were made to understand the structure–property relationship for the pervaporation dehydration membranes. Polyimides were synthesized from a hydroxyl group containing dianhydride and various diamines with methyl side groups, and the effects of substituents were studied in dehydration of ethanol aqueous solutions.[20,21] Series of polyimides membranes prepared from different dianhydrides and diamines were investigated in dehydration of ethanol/water mixtures, and the steric effects of monomer structures were discussed.[22–25] Some studies were carried out on synthesis of polyimides from monomers with functional groups, e.g., 3,5-diaminobenzoic acid (DABA), and results revealed that introduction of DABA moieties having large and hydrophilic —COOH side groups into the polymer main chains caused changes in sorption and diffusion properties.[26,27]

Pervaporation is a relatively new membrane method in separation technologies, and polyimides, similarly, have not been fully studied as materials for pervaporation membranes. Therefore, there are inadequate experimental data that can be used to find the structure–property relationship for pervaporation processes, and furthermore, the complexity of mass transport in pervaporation makes it more difficult. However, for gas separation membranes, predictions of permeabilities were successfully made by correlating the structural parameters with gas permeabilities,[28–31] which indicates that the group contribution method was an efficient tool to study membrane properties.

In our previous work, 4,4′-(hexafluoroisopropylidene) diphthalic anhydride (6FDA)-based polyimide membranes were investigated, and an empirical moiety contribution method was developed to correlate the monomer moieties of polyimides with some pervaporation parameters.[32] Because of the hydrophobicity of the 6FDA moiety, 6FDA-based polyimide membranes did not produce high selectivities towards water and isopropanol. Therefore, in this work, 2,2-bis[4-(3,4-dicarboxyphenoxy)phenyl]propane dianhydride (BPADA) was chosen as the dianhydride monomer to synthesize copolyimides with higher hydrophilicity, and the pervaporation properties were quantitatively compared with 6FDA-based membranes. Moiety contribution factors obtained from 6FDA-based membranes were utilized in calculating parameters for BPADA-based membranes, and the influences of dianhydrides and diamines were discussed in details.

EXPERIMENTAL

Materials

2,2-Bis[4-(3,4-dicarboxyphenoxy)phenyl]propane dianhydride (BPADA) was obtained from Polysciences (Warrington, PA). 4-Aminophenyl ether (ODA, 98%), 4,4′-methylenedianiline (MDA, 97%), 2,6-diaminopyridine (DAPy, 98%), 2,4-diaminobenzenesulfonic acid (DBSA, 97%), 3,5-diaminobenzoic acid (DABA, 98%), *m*-cresol (97%), isoquinoline (97%), tetrahydrofuran (THF, 99.5%), and pyridine-*d5* were supplied by Acros Organics (Morris Plains, NJ). Ethanol (99.5%), isopropanol (IPA, anhydrous, 99.5%), formamide (≥99%), diiodomethane (≥99%), and glycerol (≥ 99%) were provided by Sigma-Aldrich (Oakville, ON). Water (deionized, $\leq 2\ \mu S\,cm^{-1}$) was supplied by the Department of Chemical Engineering, University of Waterloo (Waterloo, ON). Reagents and materials were used directly as obtained.

Characterization

Polymer films were cast from THF solutions on NaCl crystals to record FTIR spectra on Bio-Rad Excalibur 3000MX spectrometer. ^{1}H-NMR spectra were recorded on Bruker 300 MHz Nuclear Magnetic Resonance Spectrometer for polymers in pyridine-*d5*. Measurement of molecular weights and molecular weight distributions were carried out on Waters Gel Permeation Chromatography (GPC) system with DAWN DSP-F Laser Photometer, Waters 2410 Refractive Index Detector, and 3 PL gel 10 μm Mixed-B columns (300 × 7.5 mm) with THF as the eluent. TA Instruments Model DSC 2920 Differential Scanning Calorimeter and Model SDT 2960 Simultaneous DSC-TGA were run for differential scanning calorimetry (DSC) analysis and thermogravimetric analysis (TGA), respectively. Samples were dried *in vacuo* at 120°C overnight before thermal analyses. DSC thermograms were recorded from 100 to 350°C and TGA from 100 to 650°C both at the heating rate of $10^{\circ}C\,min^{-1}$ in a helium atmosphere. DSC curves were plotted with a baseline obtained from a DSC run with an empty aluminum sample pan. Contact angles of polymer membranes were calculated from images taken on Tantec Contact Angle Meter (U.S.

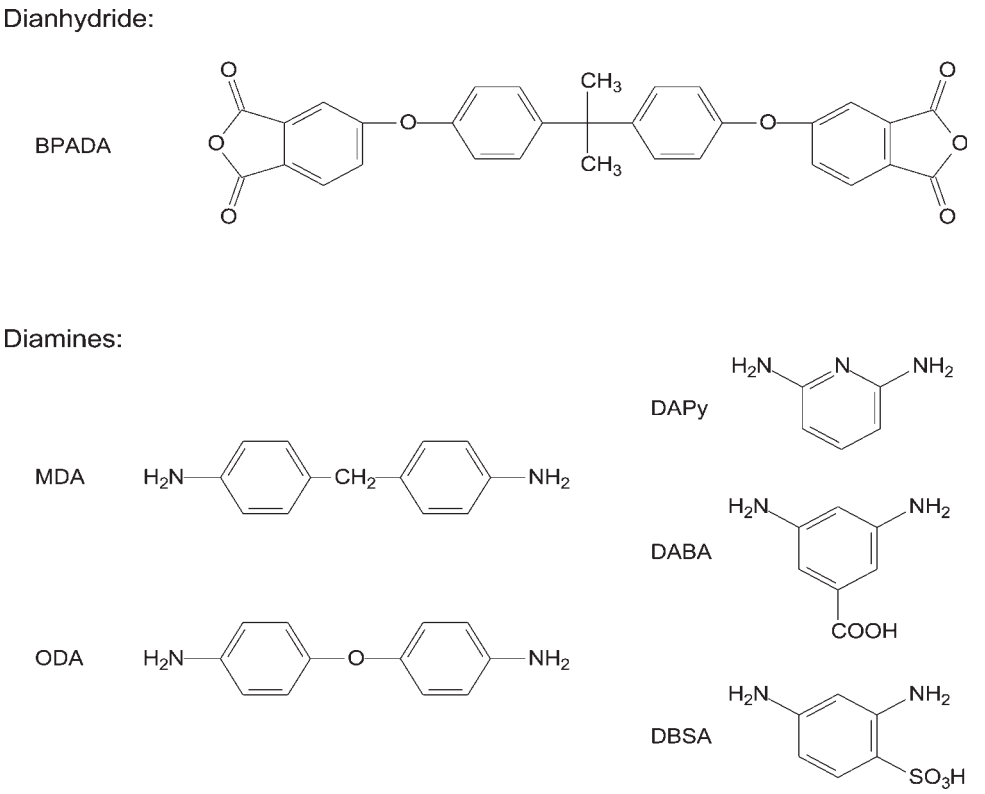

Figure 1 Chemical structures of monomers.

Patent 5,268,733) with four liquids, i.e., water, glycerol, formamide, and diiodomethane, at room temperature.

Synthesis of polymers

BPADA-based polyimides were synthezied from the monomers shown in Figure 1. DAPy, DABA, and DBSA were used as the third monomers in the copolyimides. The polyimides (listed in Table I) were synthesized from one-step polymerization, and procedures are outlined as follows, BPADA-8ODA-2DAPy as an example:

BPADA 2.082 g (4 mmol), ODA 0.654 g (3.2 mmol), and DAPy 0.089 g (0.8 mmol) were charged into a 100 mL three-neck flask with a mechanical stirrer, a Dean-Stark trap, a condenser, and nitrogen inlet/outlet. Fresh 17 mL *m*-cresol was added into the flask to afford a concentration of 16 w/v %. A catalytical amount of isoquinoline and 2 mL *m*-cresol were also charged into the system. The mixture formed a solution and reacted at 75°C for 2 h. Then, the temperature was slowly increased to 185°C. Polymerization lasted for 20–24 h. During this period, 2 mL *m*-cresol was distilled out through the trap. The viscous solution was cooled to below 120°C and was precipitated into an excess of ethanol to get the white polymer. The obtained polymer was collected and washed with ethanol in a Soxhlet extractor to remove the solvent for at least 12 h. The final product BPADA-8ODA-2DAPy was dried under an infrared lamp first, then *in vacuo* at 150°C for 20 h.

TABLE I
Synthesis of BPADA Copolyimides and Molecular Weights

Polyimides	Monomers	Molar ratio	$\overline{M}_n$	$\overline{M}_w$	$\overline{M}_w/\overline{M}_n$	$\overline{DP}$
BPADA-ODA	BPADA : ODA	1 : 1	65,840	87,500	1.33	96
BPADA-8ODA-2DAPy	BPADA : ODA : DAPy	1 : 0.8 : 0.2	57,990	74,960	1.29	87
BPADA-8ODA-2DABA	BPADA : ODA : DABA	1 : 0.8 : 0.2	141,900	163,800	1.15	210
BPADA-8ODA-2DBSA	BPADA : ODA : DBSA	1 : 0.8 : 0.2	197,900	237,500	1.20	290
BPADA-MDA	BPADA : MDA	1 : 1	70,430	93,810	1.33	103
BPADA-8MDA-2DAPy	BPADA : MDA : DAPy	1 : 0.8 : 0.2	75,840	108,900	1.44	114
BPADA-8MDA-2DABA[a]	BPADA : MDA : DABA	1 : 0.8 : 0.2	–	–	–	–
BPADA-8MDA-2DBSA[a]	BPADA : MDA : DBSA	1 : 0.8 : 0.2	–	–	–	–

[a] Poor mechanical properties and low molecular weights, and no further tests were carried out.

In addition to BPADA-8ODA-2DAPy, two polyimides BPADA-ODA and BPADA-MDA, as well as three copolymers BPADA-8ODA-2DABA, BPADA-8ODA-2DBSA, and BPADA-8MDA-2DAPy, were successfully prepared from the procedures described earlier. BPADA-8MDA-2DABA and BPADA-8MDA-2DBSA showed low molecular weights and could not be used for further research.

BPADA-ODA (film, cm^{-1}): 3481(vw) ν_{as} N—H, 3061(br, w) aromatic δ C—H, 2976(m) ν_{as} CH_3, 2870(br, w) ν_s CH_3, 1776(m) ν_{as} C=O, 1716(s) ν_s C=O, 1599(br, m) phenyl ring, 1502(s) phenyl ring, 1444(m) ν_{as} CH_3, 1381(m) ν C—N, 1276(m) ν C—N amide, 1238(br, m) ν_{as} C—O—C, 1078(br, m) imide, 1014(m) aromatic δ C—H, 744(m) δ imide. ^{1}H-NMR (Pyridine-*d5*, δ ppm): 7.97-7.94 (1.9H), 7.77-7.74 (3.7H), 7.66-7.65 (2.0H), 7.48-7.41 (6.2H), 7.29-7.24 (4.0H), ~ 7.22 (theoretically 4.0H, overlapped), 1.75 (6.0H).

BPADA-8ODA-2DAPy (film, cm^{-1}): 3483(w) ν_{as} N—H, 3053(br, m) aromatic δ C—H, 2978(m) ν_{as} CH_3, 2854(br, w) ν_s CH_3, 1776(m) ν_{as} C=O, 1720(s) ν_s C=O, 1599(br, m) aromatic ring, 1502(br, s) aromatic ring, 1445(m) ν_{as} CH_3, 1381(m) ν C—N, 1278(m) ν C—N amide, 1242(br, m) ν_{as} C—O—C, 1068(br, m) imide, 1014(m) aromatic δ C—H, 744(m) δ imide. ^{1}H-NMR (Pyridine-*d5*, δ ppm): 7.97-7.87 (2.0H), 7.81-7.74 (3.6H), 7.66-7.65 (1.6H), 7.48-7.41 (6.2H), 7.29-7.24 (theoretically 7.2H, overlapped), 1.75 (6.4H).

BPADA-8ODA-2DABA (film, cm^{-1}): 3481(vw) ν_{as} N—H, 3057(br, w) aromatic δ C—H, 2974(m) ν_{as} CH_3, 2868(br, w) ν_s CH_3, 1776(m) ν_{as} C=O, 1722(s) ν_s C=O, 1598(br, m) phenyl ring, 1504(br, s) phenyl ring, 1446(m) ν_{as} CH_3, 1381(m) ν C—N, 1276(m) ν C—N amide, 1242(br, m) ν_{as} C—O—C, 1078(br, m) imide, 1015(m) aromatic δ C—H, 744(m) δ imide. ^{1}H-NMR (Pyridine-*d5*, δ ppm): 8.83 (0.2H), 8.14-8.19 (0.1H), 7.97-7.94 (2.0H), 7.77-7.74 (3.2H), 7.66-7.65 (2.0H), 7.48-7.41 (6.6H), 7.29-7.24 (theoretically 7.2H, overlapped), 1.75 (6.4H).

BPADA-8ODA-2DBSA (film, cm^{-1}): 3481(vw) ν_{as} N—H, 3053(br, w) aromatic δ C-H, 2974(m) ν_{as} CH_3, 2872(br, w) ν_s CH_3, 1778(m) ν_{as} C=O, 1722(s) ν_s C=O, 1600(br, m) phenyl ring, 1502(br, s) phenyl ring, 1446(m) ν_{as} CH_3, 1379(m) ν C—N, 1276(m) ν C—N amide, 1240(br, m) ν_{as} C—O—C, 1078(br, m) imide, 1015(m) aromatic δ C—H, 744(m) δ imide. ^{1}H-NMR (Pyridine-*d5*, δ ppm): 8.28 (0.1H), 7.97-7.91 (1.9H), 7.84-7.81 (0.4H), 7.77-7.74 (3.1H), 7.66-7.63 (2.1H), 7.48-7.41 (6.1H), 7.29-7.24 (theoretically 7.1H, overlapped), 1.75 (6.0H).

BPADA-MDA (film, cm^{-1}): 3481(vw) ν_{as} N—H, 3039(br, w) aromatic δ C—H, 2976(m) ν_{as} CH_3, 2868(br, w) ν_s CH_3, 1776(m) ν_{as} C=O, 1716(s) ν_s C=O, 1601(br, m) phenyl ring, 1514(br, m) phenyl ring, 1446(m) ν_{as} CH_3, 1373(m) ν C—N, 1276(m) ν C—N amide, 1240(br, m) ν_{as} C—O—C, 1068(br, m) imide, 1015(m) aromatic δ C—H, 744(m) δ imide. ^{1}H-NMR (Pyridine-*d5*, δ ppm): 7.95-7.92 (2.0H), 7.71-7.68 (4.0H), 7.65-7.64 (1.9H), 7.46-7.37 (10.2H), 7.28-7.26 (theoretically 4.0H, overlapped), 4.02 (1.8H), 1.74 (6.1H).

BPADA-8MDA-2DAPy (film, cm^{-1}): 3481(vw) ν_{as} N—H, 3039(br, w) aromatic δ C-H, 2976(m) ν_{as} CH_3, 2860(br, w) ν_s CH_3, 1776(m) ν_{as} C=O, 1722(s) ν_s C=O, 1599(br, m) aromatic ring, 1512(br, m) aromatic ring, 1445(m) ν_{as} CH_3, 1375(m) ν C—N, 1275(m) ν C—N amide, 1238(br, m) ν_{as} C—O—C, 1067(br, m) imide, 1015(m) aromatic δ C—H, 744(m) δ imide. ^{1}H-NMR (Pyridine-*d5*, δ ppm): 7.95-7.87 (2.0H), 7.81-7.78 (0.4H), 7.71-7.68 (3.2H), 7.64-7.63 (1.6H), 7.46-7.37 (9.6H), 7.28-7.24 (theoretically 4.0H, overlapped), 4.02 (1.5H), 1.74 (6.2H).

Dense membrane preparation

Polymers were readily dissolved in THF, and the obtained 5 w/v % polyimide solutions were filtered with Target PTFE syringe filters (National Scientific, pore size 0.45 μm). Polymer solutions were cast on clean and smooth glass plates and kept in a dry clean chamber for at least 4 h. The slow evaporation rate of THF was required to form good membranes. To prevent possible defects in the membranes, polymer solutions were cast onto the dried membranes on the glass plates 2–4 times. Thickness of membranes was measured with a micrometer to be 15–25 μm. Membranes were peeled off the glass plates and were ready to use.

Pervaporation processes

Temperature and concentration effects on pervaporation properties were studied for dehydration of isopropanol in this work. To investigate the temperature dependence of flux and selectivity, feed water contents were kept to be ~ 20 wt %, and feed temperatures were controlled to vary from 30 to 70°C. The effects of the feed concentration on separation performances were studied by changing the feed water content from ~ 10 to ~ 50 wt %, while the operating temperature was remained at 60°C. The feed temperatures were controlled within ±0.2°C with a heating mantle, the Dyna-Sense Thermoregulator Control System, a thermometer, and a circulation pump. Vacuum (<300 Pa absolute) was applied to the permeation side. Permeates were collected in cold traps with liquid nitrogen. At least 1 h operation was conducted to attain the steady state before collecting permeates for analysis. Feed and permeate concentrations were determined by a Varian CP-3800 Gas Chromatograph. Permeation flux J is defined by the following equation:

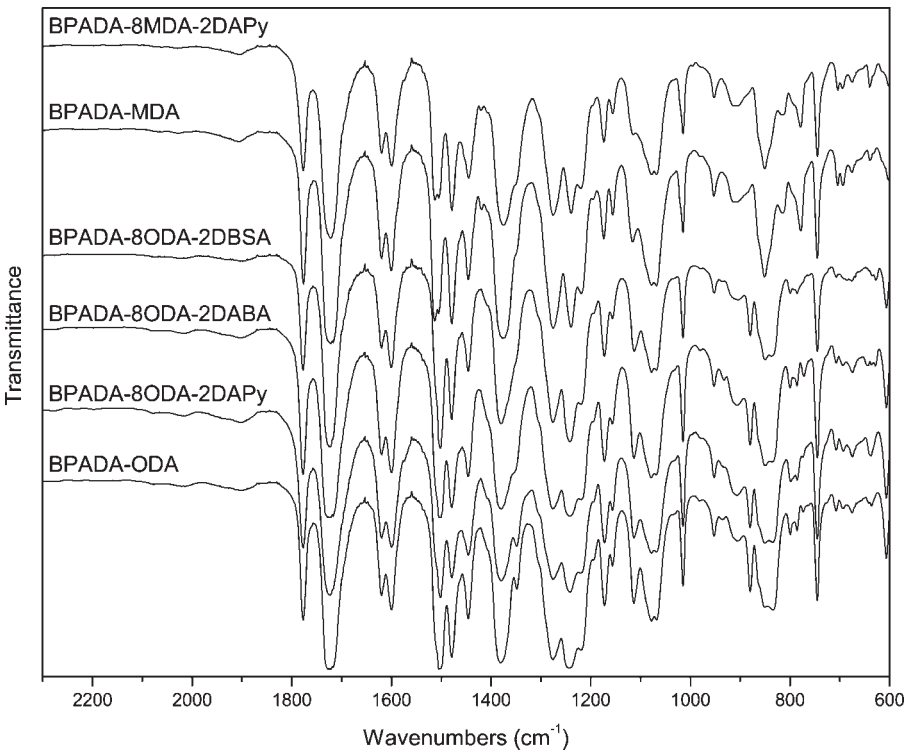

Figure 2 FTIR spectra of polyimides.

$$J = \frac{Q}{S\,t} \tag{1}$$

where Q, S, t are total amount of permeate, effective membrane area, and operating time, respectively.

RESULTS AND DISCUSSION

BPADA-based polyimides

The dianhydride monomer BPADA was used to react with diamine monomers in *m*-cresol at elevated temperatures in the presence of isoquinoline. Among the diamine monomers, DAPy, DABA, and DBSA were used as the third monomers to prepare BPADA-ODA-based and BPADA-MDA-based copolymers. Although poly(amic acid)s were formed in the first stage of the polymerization at the lower temperature ($\sim$ 80°C), the lengths of the linear polymer chains still increase when the reaction temperature was increased to $\sim$ 180°C. This is different from the conventional two-step polymerization of polyimides where the molecular weight of the final product mainly depends on that of the precursor poly(amic acid). It failed to obtain BPADA-8MDA-2DABA and BPADA-8MDA-2DBSA films with good mechanical properties from this method, and no further tests were conducted for these two polymers. Table I shows molecular weights of the polyimides, degrees of polymerization and their molecular weight distributions. BPADA-8ODA-2DABA and BPADA-8ODA-2DBSA have higher molecular weights than the others. The molecular weight distributions vary in the range of 1.15–1.44. The small values of $\overline{M}_w/\overline{M}_n$ obtained from GPC result from the fractionation effect of the ethanol during the extraction of *m*-cresol.

In FTIR spectra of the polyimides, the absorption peak of N—H asymmetrical stretching vibration can be observed at 3481 cm^{-1}, and the absorption of aromatic C—H bending vibration occurs at $\sim$ 3050 cm^{-1}.[33] Figure 2 shows FTIR spectra of the polymers in the range of 2300–600 cm^{-1}. The absorption peaks of skeletal vibrations, involving carbon–carbon stretching within the phenyl ring appear at $\sim$ 1600 and $\sim$ 1500 cm^{-1}. The in-plane bending of C—H on the phenyl rings show a peak at 1014 cm^{-1}. The imide I band at 1776 cm^{-1} (C=O asymmetrical stretching), imide II band at 1722 cm^{-1} (C=O symmetrical stretching), imide III band at $\sim$ 1078 cm^{-1}, and imide IV band at 744 cm^{-1} (imide ring bending vibration) occur in all FTIR spectra of BPADA-based polyimides.[34,35] The peaks at $\sim$ 1380 and $\sim$ 605 cm^{-1} are also attributed to the imide structure of the polymers.[35,36] The asymmetrical stretching vibration of aryl aryl ether produces absorption at 1240 cm^{-1}, and the absorption at 1276 cm^{-1} is probably due to the stretching vibration of C—N in the unreacted amide groups.[37]

Figure 3 shows the ^{1}H-NMR of BPADA-MDA. Protons in —CH_2 and —CH_3 groups have chemical

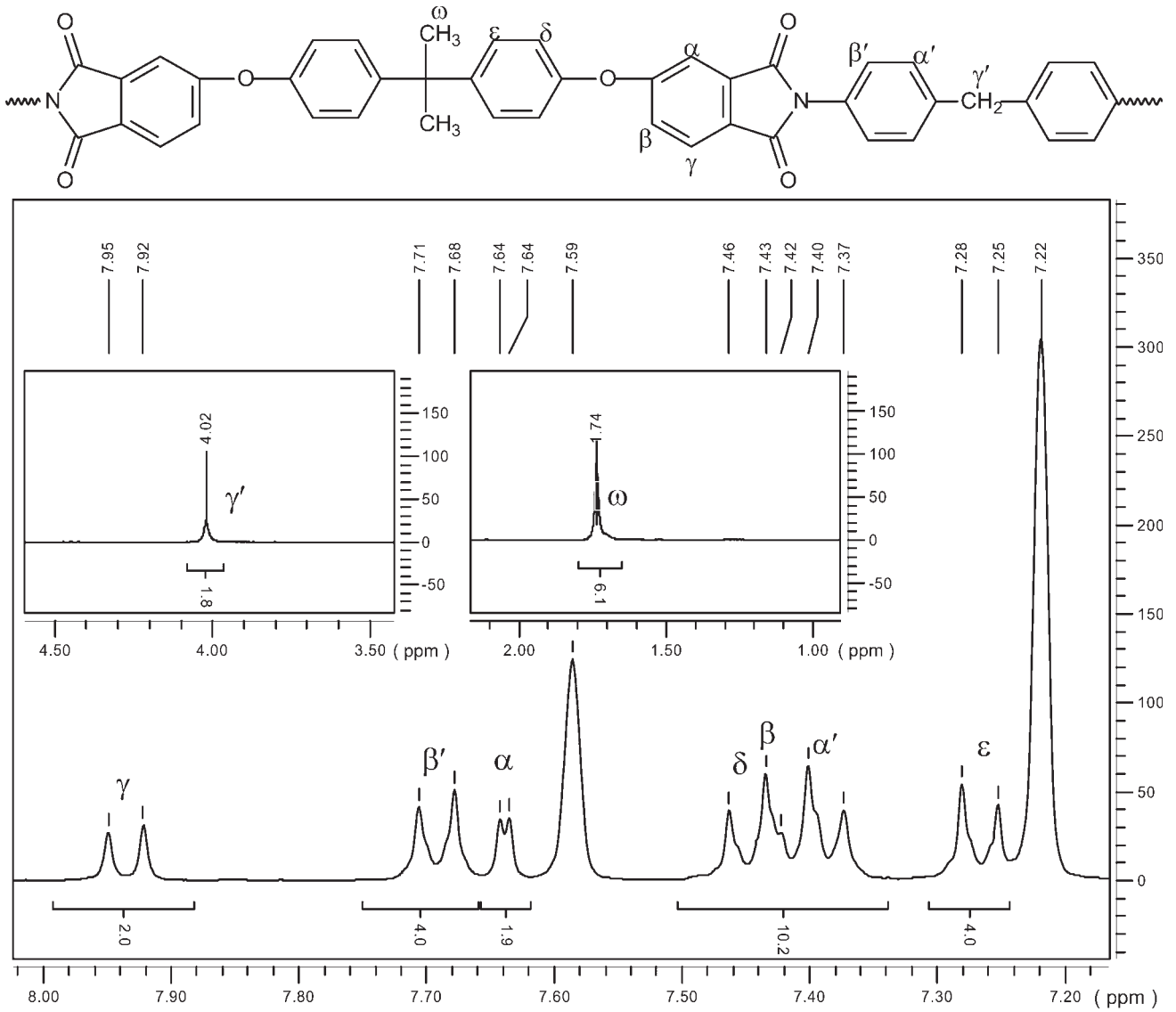

Figure 3 ^{1}H-NMR of BPADA-MDA.

shifts of 4.02 and 1.74 ppm, respectively. $H_{\alpha'}$ and $H_{\beta'}$ are correlated, and H_δ couples with H_ε. The two protons, H_β and H_γ, are located on adjacent C atoms, and furthermore, H_β is overlapped by H_δ and H_α. H_α shows no coupling relationship with other protons, and its chemical shift is 7.64 ppm. Figure 4 shows ^{1}H-NMR spectra of all BPADA-based polyimides. Compared with the BPADA-MDA and its proton assignment in Figure 3, the two protons of DAPy moieties in BPADA-8MDA-2DAPy can be identified to show peaks at 7.80 and ~ 7.40 ppm. Different from BPADA-MDA, the two protons of ODA moieties in the BPADA-ODA spectrum have chemical shifts of 7.75 and ~ 7.24 ppm, respectively. Accordingly, from the coupling relationships and integration properties, chemical shifts can be assigned to different protons of DAPy moieties in BPADA-8ODA-2DAPy, protons of DABA moieties in BPADA-8ODA-2DABA and protons of DBSA moieties in BPADA-8ODA-2DBSA: ~ 7.77 and ~ 7.41 ppm for DAPy, 8.83 and 8.11 ppm for DABA, 8.28, 7.84, and 7.81 ppm for DBSA, respectively.

Properties of polyimides

Solubility

Solubility of the polyimides was tested by putting small pieces of polyimides into large amounts of solvents. All polymers are readily soluble in THF and pyridine, and they can get dissolved in chloroform, *N,N*-dimethylacetamide (DMAc), *N,N*-dimethylformamide (DMF), *N*-methylpyrrolidone (NMP) and dimethyl sulfoxide (DMSO), but they are insoluble in isopropanol, acetone, toluene and cyclohexane.

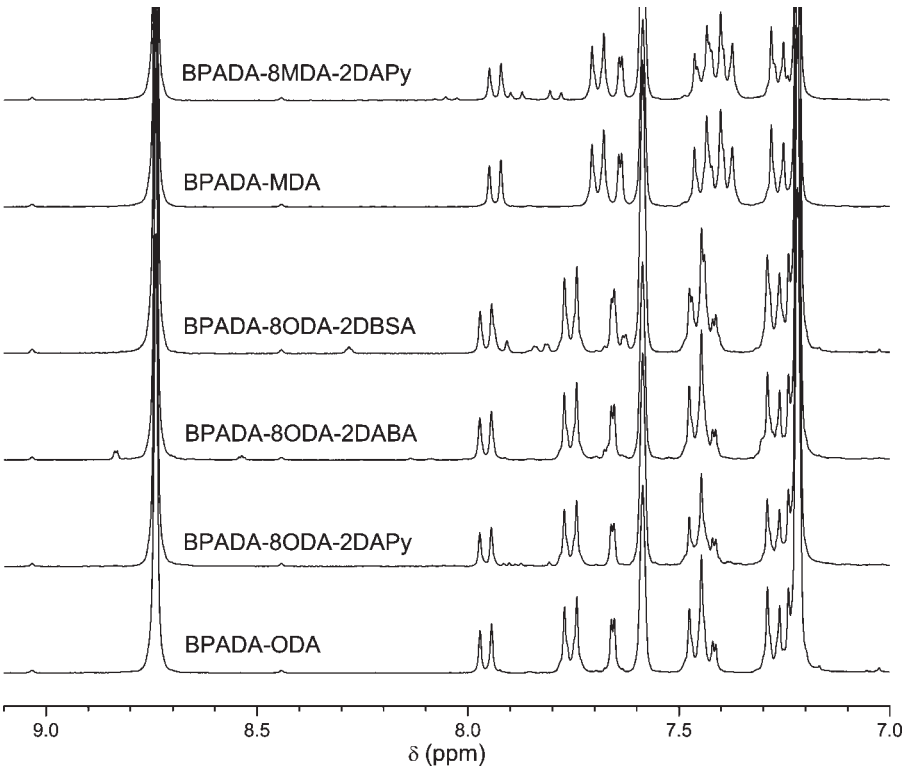

Figure 4 ^{1}H-NMR spectra of BPADA-based polyimides.

Thermal properties

Readings of the DSC curves are presented in Table II. No distinct transitions can be observed in the first or the second DSC runs for the polyimides, but only tiny slope changes of the curves can be found if the curves are drawn using the DSC trace of an empty sample pan as the baseline. The DSC temperatures in Table II were read as DSC onset temperatures, and they are used as an estimation of the glass transition temperatures. According to the known T_gs of BPADA-ODA (215°C), BPADA-MDA (217°C),[38] the estimated temperatures in Table II are reasonably comparable. A sequence can be seen in the DSC onset temperatures of BPADA-ODA-based polyimides: BPADA-8ODA-2DAPy > BPADA-8ODA-2DABA > BPADA-8ODA-2DBSA > BPADA-ODA. It results in a sequence of the contributions from diamines to the glass transition temperatures: DAPy > DABA > DBSA > ODA. The flexible ether bonds in ODA moieties can decrease T_g, so the lowest onset temperature is observed for BPADA-ODA. The side groups of —COOH in DABA moieties and —SO_3H groups in DBSA moieties may change the

TABLE II
Readings of DSC, TGA, and DTG Curves and Estimated Apparent Activation Energies for Thermal Decomposition

Polyimides	DSC[a] (°C)	T_d 5% wt. loss (°C)	T_d 10% wt. loss (°C)	T_d onset[b] (°C)	DTG[c] (°C)	E_d[d] (kJ mol^{-1})
BPADA-ODA	218.9	517.0	530.6	521.8	542.6	350
BPADA-8ODA-2DAPy	234.1	507.8	522.2	511.6	535.9	300
BPADA-8ODA-2DABA	228.7	480.9	517.1	~ 350[e]	420.3[e]	–
				508.1	536.8	260
BPADA-8ODA-2DBSA	225.2	519.8	531.2	524.3	542.4	380
BPADA-MDA	225.8	489.5	512.0	500.0	527.9	250
BPADA-8MDA-2DAPy	228.5	485.1	504.4	492.1	523.5	190

[a] DSC operating conditions: 10°C min^{-1} in helium. Glass transition temperatures were not distinctly decided from the first and second runs of DSC. The onset temperatures were used as an estimation of their glass transition temperatures.
[b] TGA operating conditions: 10°C min^{-1} in helium.
[c] These temperatures were read as DTG peak temperatures.
[d] Estimated apparent activation energies for thermal decomposition in the range of ~ 520–550°C.
[e] BPADA-8ODA-2DABA showed two degradation stages in TGA. This temperature was obtained from the first-stage degradation.

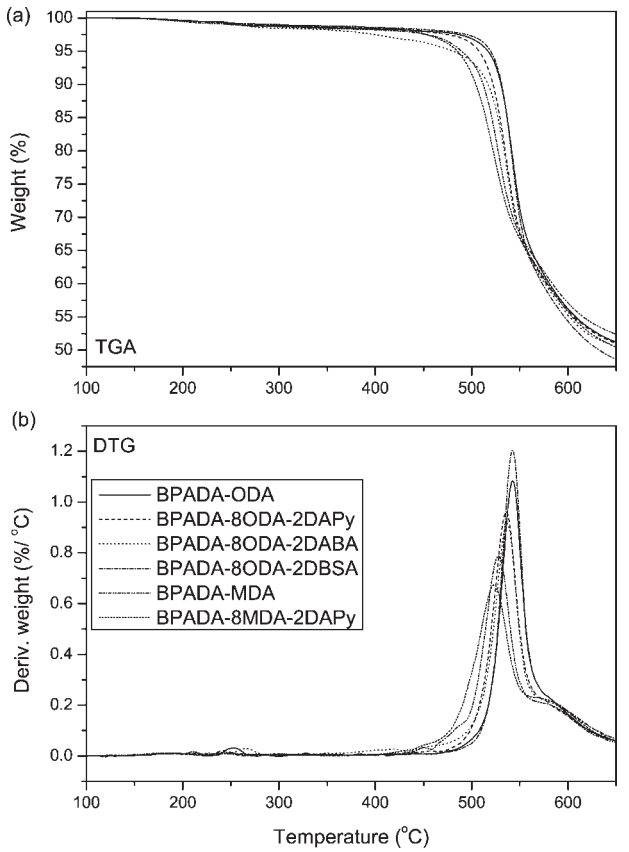

Figure 5 TGA (a) and DTG (b) curves of polyimides.

uniformity and the packing density of polymer matrices, and can slightly lower the T_gs.

TGA and DTG curves of the polyimides are displayed in Figure 5, and readings from the curves are listed in Table II. BPADA-8ODA-2DABA undergoes two stages of degradation starting from $\sim$ 350 and $\sim$ 500°C, respectively, and it has lower T_ds for 5% and 10% weight losses.

The values of the apparent activation energies for thermal decomposition were calculated from the Broido equation,[39] and the results are listed in Table II. It is observed that all TGA curves pass though the point of (560°C, 64%). The polymers with larger values of the decomposition activation energy appear to have a higher degradation rate when the temperature approaches 560°C, and hence these polymers have better thermal stability below 560°C. The significant difference in the values of activation energies reduces the possible error when these data are compared.

Surface free energies

Measurements of contact angles of a drop of liquid resting on a horizontal membrane surface (a sessile drop) were made at room temperature by capturing the digital images of the droplets, followed by analysis of their shapes. Contact angles of sessile drops of liquids on BPADA-based polyimides are listed in Table III.

Contact angles are studied to understand the wetting properties of a solid surface in terms of the Young equation[40]:

$$\cos\theta = \frac{\gamma_{sv} - \gamma_{sl}}{\gamma_{lv}} \tag{2}$$

where θ is the contact angle of the liquid l on the surface of solid s, γ_{sv} is the surface free energy of the solid in equilibrium with the saturated vapor of the liquid, γ_{lv} is the surface free tension of the liquid in equilibrium with the solid, and γ_{sl} is the solid–liquid interfacial free energy. Following the suggested form of surface free energy by Fowkes, van Oss et al. defined the surface free energy as the sum of the Lifshitz-van der Waals apolar (LW) component γ_i^{LW} and the Lewis acid-base (AB) component γ_i^{AB}.[40]

$$\gamma_i = \gamma_i^{LW} + \gamma_i^{AB} \tag{3}$$

The Lewis theory was utilized to deal with acid-base interactions where hydrogen bonding, π-bonds, and ligand formation may be involved in a bipolar system. The acid–base component γ_i^{AB} was split into two mono-polar surface parameters: Lewis acid (electron-acceptor) subcomponent γ^+ and Lewis base (electron-donor) subcomponent γ^-. The substance i is considered to be apolar if both the acidic and

TABLE III
Contact Angles of Liquids on Polyimide Membranes from the Sessile Drop Method

Membranes	Water (°)	Glycerol (°)	Formamide (°)	Diiodomethane (°)
BPADA-ODA	83.6 ± 0.3	67.2 ± 0.3	57.4 ± 2.0	23.3 ± 1.0
BPADA-8ODA-2DAPy	77.7 ± 0.8	62.6 ± 0.5	56.8 ± 0.6	17.6 ± 0.9
BPADA-8ODA-2DABA	84.2 ± 0.8	60.5 ± 1.0	54.7 ± 1.4	19.8 ± 1.8
BPADA-8ODA-2DBSA	78.7 ± 1.0	65.8 ± 1.4	56.5 ± 0.6	19.9 ± 1.1
BPADA-MDA	70.2 ± 1.5	61.7 ± 1.0	52.4 ± 1.2	20.3 ± 1.0
BPADA-8MDA-2DAPy	82.2 ± 1.6	64.4 ± 0.4	55.2 ± 0.9	31.6 ± 0.8

All results are given as means with 95% confidence intervals.

TABLE IV
Surface Free Energy Components ($mJ\,m^{-2}$) and Membrane–Water Interfacial Free Energies ($mJ\,m^{-2}$) of Polyimides

Membranes	γ_s^{LW}	γ_s^+	γ_s^-	γ_s^{AB}	γ_s	ΔG_{sw}^{IF}
BPADA-ODA	46.74	0.0043	2.66	0.21	46.96	−77.54
BPADA-8ODA-2DAPy	48.45	0.0001	5.25	0.05	48.50	−66.22
BPADA-8ODA-2DABA	47.84	0.2187	1.18	1.02	48.86	−82.71
BPADA-8ODA-2DBSA	47.81	0.0001	4.68	0.04	47.86	−68.40
BPADA-MDA	47.69	0.0001	10.31	0.06	47.76	−47.14
BPADA-8MDA-2DAPy	43.55	0.1897	2.74	1.44	44.99	−70.09

basic subcomponents are negligible, such as diiodomethane (DIM).[40]

$$\gamma_i^{AB} = 2\sqrt{\gamma_i^- \gamma_i^+} \tag{4}$$

The Lifshitz-van der Waals component γ_i^{LW} is the apolar component associated with Lifshitz-van der Waals interactions including London dispersion forces, Debye-polarization, and Keesom forces, and it can be determined from measurement of the contact angles of an apolar liquid on the solid surface. In this work, γ_s^{LW} values of the membranes were calculated from contact angles by using diiodomethane.[41,42]

$$\gamma_s^{LW} = \frac{\gamma_{DIM}^{LW}(1 + \cos\,\theta_{DIM})^2}{4} \tag{5}$$

The two subcomponents of γ_s^{AB} can be determined with the following equation from the contact angles of at least two liquids.[42]

$$\gamma_l(1 + \cos\theta) = 2\left(\sqrt{\gamma_s^{LW}\gamma_l^{LW}} + \sqrt{\gamma_s^+\gamma_l^-} + \sqrt{\gamma_s^-\gamma_l^+}\right) \tag{6}$$

Water, glycerol, and formamide were applied in the measurement of contact angles on the polyimide membranes. Thus, the subcomponent of γ_s^{AB} and total surface free energy γ_s can be decided for membranes according to eqs. (5) and (6), respectively. The free energy of the interfacial interaction between the membrane and water can be obtained from the following equation:

$$\Delta G_{sw}^{IF} = -2\left(\sqrt{\gamma_s^{LW}} - \sqrt{\gamma_w^{LW}}\right)^2 - 4\left(\sqrt{\gamma_s^+\gamma_s^-} + \sqrt{\gamma_w^+\gamma_w^-} - \sqrt{\gamma_s^+\gamma_w^-} - \sqrt{\gamma_s^-\gamma_w^+}\right) \tag{7}$$

Table IV exhibits the results of the calculations above from contact angles measured with standard liquids. The values of contact angles of the polyimide membranes are found in an order: water > glycerol > formamide ≫ diiodomethane. Since diiodomethane is considered as an apolar liquid, the smaller values of contact angles reflect more affinity of the polyimides to the apolar liquid.

The total surface energies γ_s of the polyimides vary in the range of 45–49 mJ m^{-2}. The LW components of surface free energies γ_s^{LW} appear between 43.5 and 48.5 $mJ\,m^{-2}$, and are predominantly greater than the AB components γ_s^{AB}, which is related to the less polarity of the polymer. Looking at the subcomponents of γ_s^{AB}, it can be found that some γ_s^+ values are close to zero, but γ_s^- values are much larger. This electron-donicity is suggested to result from the interactions between electron donating and accepting sites (Lewis neutralization) as well as the residual hydration,[43] and the hydrophilicity can be correlated with γ_s^-,[44] but for polyimide membranes, the Lewis base components γ_s^- are probably influenced by the basicity of the polyimides from their residual amino groups.

The free energy of the interfacial interaction combines the surface properties of the liquid and the solid. In the water-membrane systems, the values of ΔG_{sw}^{IF} can be used directly to compare the hydrophilicity of the membranes. It is known that hydrophobic membranes exhibit negative values, and when immersed in water, their surfaces prefer to be in contact with each other rather than forming an interface with water.[45] Therefore, BPADA-MDA shows to be more hydrophilic than the others, which is consistent with the results of contact angles and the values of γ_s^-.

Pervaporation properties

According to the solution–diffusion model, sorption of the penetrants occurs at the upstream surface of the membrane, and the sorbed species diffuse across the membrane with the driving force of chemical potential difference between the upstream and the downstream surfaces. The penetrants evaporate at the downstream surface to form vaporous permeates. Evaporation (or desorption from the membrane) of permeates is usually considered to be very fast, and therefore, permeation of the penetrants is generally determined by sorption and diffusion

properties. The following relationship is determined from the solution-diffusion model:

$$P_i = S_i D_i \quad (8)$$

where P_i is the permeability coefficient, S_i is the solubility coefficient, and D_i is the diffusivity coefficient.

Effects of monomer moieties

Pervaporation membranes are nonporous membranes, and no apparent paths can be observed for penetrants in the membranes. Diffusion of the penetrants is facilitated by the thermal agitated movements of the segmental polymer chains. Transient gaps are formed and the penetrant molecules hop between the gaps from the upstream side of higher chemical potentials to the downstream side of lower chemical potentials.[46] The transient gaps are related to the free volume in free volume theory. At a temperature below T_g, polymers are in the glassy state, and the mobility of the polymer chains is greatly limited. Therefore, the polymer matrix of a glassy polymer can be considered as a finely organized "molecular sieve" for the penetrants. On the one hand, water molecules can pass through the membrane more easily than isopropanol molecules, in pervaporation of water/isopropanol, because the kenetic diameter of water (0.265 nm) is much smaller than that of isopropanol (0.43 nm).[47,48] On the other hand, structural units of the polymer control the size of the transient gaps, and the differences in diffusivity selectivities of water/isopropanol can be predicted for the membranes prepared from different monomers. A flexible structure can produce more "space" than a rigid unit, and furthermore, bulky side groups are helpful to decrease the packing density of the polymer chains and generate wider gaps for the penetrants to pass through.

Besides the diffusion properties of the penetrants in membranes, according to eq. 8, sorption of penetrants probably plays a more significant role in deciding permeability of a pervaporation membrane. Sorption is the effect of penetrant molecules incorporated into the polymer matrix, including bonding of ions and physical adherence to the polymer chains.[49] The sorbed species have higher chemical potentials at the surface in contact with the feed, and hence the diffusion driving forces are formed across the membrane. More "free space" in the polymer matrix and a smaller size of the penetrants are favorable to better sorption. In addition, interactions between the penetrants and the polymer matrix can affect sorption properties, and possibly have influence on diffusion properties as well.

BPADA is a dianhydride monomer with a long structure, and the isopropylene structure and the ether bonds between phenyl rings make the moieties flexible in BPADA-based polyimides. If comparison is made between BPADA and 6FDA moieties, the structure of BPADA is more flexible than that of 6FDA, though 6FDA bears the flexible hexafluoroisopropylidene moiety.[32] However, the $—CF_3$ groups in 6FDA are much larger than $—CH_3$ groups in BPADA, and 6FDA moieties may also be favorable to the sorption and diffusion of the penetrants. In addition, because of the existence of the extra oxyphenyl moieties, the distribution concentration of BPADA in BPADA-based membranes is higher than that of 6FDA in 6FDA-based membranes. Therefore, the structural effects from other moieties within the polymer chains are reduced in BPADA-based polyimides. The imide rings are hydrophilic because hydrogen bonding can be formed between water and acyl groups, but their affinity to water can be reduced by the hydrophobicity of $—CH_3$ groups in BPADA and $—CF_3$ groups in 6FDA.

ODA an MDA have similar structures, but the methylene group in MDA is more flexible than the ether bond in ODA, so the diffusivity of penetrants in BPADA-MDA should be higher than that in BPADA-ODA. DAPy, DABA, and DBSA are much smaller in size than ODA and MDA, and introduction of these moieties into BPADA-MDA or BPADA-ODA may cause an increase in distribution concentration of BPADA moieties. Moreover, the side groups of —COOH and $—SO_3H$ in DABA and DBSA, respectively, can lead to higher diffusivity of water and isopropanol as well as better sorption of water, due to their steric effects and hydrophilicity.[32] The lone electron pair in DAPy moiety may have some interactions with isopropanol, and is helpful to increase the permeation of isopropanol.

Effects of feed concentrations

Pervaporation dehydration of isopropanol was carried at 60°C, and the feed water contents varied between 10 and 50 wt %. Permeation flux and permeate water contents are presented in Figure 6.

It is observed that with an increase in the feed water content, most of the membranes have higher permeate water contents, and a similar tendency can be seen in permeation flux. These results are mainly attributed to the enhancement of water sorption in the polymer matrix. Furthermore, when water is sorbed in the matrix, it may cause an expansion of the matrix, especially for glassy polymers with flexible structures, which may be a reason why at the feed water contents of 10–30 wt %, an increase in flux and a decrease in the permeate water content occur for BPADA-ODA membrane. BPADA-8ODA-

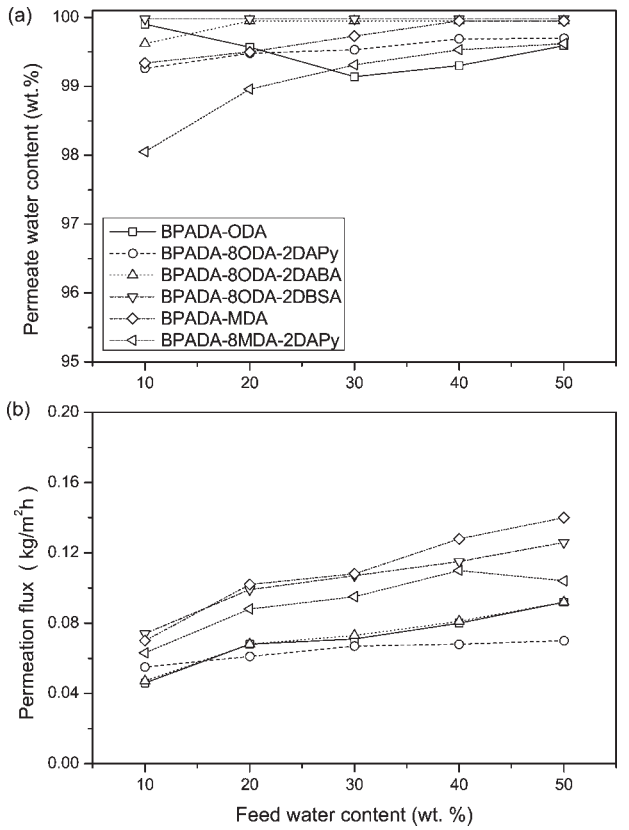

Figure 6 Permeation flux and permeate water contents for pervaporation dehydration of isopropanol at 60°C.

2DBSA and BPADA-8ODA-2DABA membranes have good selectivity for water/isopropanol, benefiting from the hydrophilicity of their functional groups. With the possible affinity to isopropanol, polyimides containing DAPy moieties show worse selectivity for water/isopropanol. Because of the flexibility of MDA moieties, BPADA-MDA and BPADA-8MDA-2DAPy yield higher flux and higher isopropanol contents in the permeates.

Permeation flux is dependent on the membrane thickness, and the increasing rate of flux can be obtained and work for the comparison of flux or further studies.[32] Based on experimental data, from curve fitting, an empirical equation was developed for the effects of the feed concentration on total flux and water flux in the permeates.[32]

$$J(x_w) = k\,x_w^n \tag{9}$$

where $J(x_w)$ is the permeation flux at the feed water content of $x_w \times 100$ wt %, n is defined as the "concentration coefficient" for the membrane at 60°C. k is a parameter related to membrane properties as well as operating conditions, and it can be considered as a constant for the same membrane at the same temperature.

The n values were determined from total flux and water flux of the same membranes from curving fitting, and the calculated n values are listed in Table V. For the purpose of comparison, the n values of 6FDA-based polyimide membranes are also listed in Table V.[32]

Since BPADA-based polyimide membranes produced permeates of high water contents, the n values for total flux and water flux are very close. Compared with 6FDA-based polyimide membranes, most of BPADA-based polyimides have larger n values. The hydrophobicity of 6FDA moieties and the flexibility of BPADA moieties contribute to these differences. It should be noted that BPADA-8ODA-2DAPy has exceptional n values, possibly resulting from the high thickness of the membrane, because greater resistance and lower degree of expansion of the thick membrane can reduce the permeation flux with the higher water contents in the feed. So, a question was raised, could the reasonable n values of BPADA-8ODA-2DAPy be predicted from the n

TABLE V
Comparison of Concentration Coefficients and Permeation Activation Energies for BPADA-Based Membranes and 6FDA-Based Membranes

	n		E_p (kJ mol^{-1})	
Membranes	Total flux	Water flux	Total flux	Water flux
BPADA-ODA	0.43	0.4	37.9	37.6
BPADA-8ODA-2DAPy	0.18	0.18	38.6	38.6
BPADA-8ODA-2DABA	0.41	0.41	52.1	52.2
BPADA-8ODA-2DBSA	0.34	0.34	45.7	45.9
BPADA-MDA	0.43	0.43	55.6	55.7
BPADA-8MDA-2DAPy	0.44	0.45	36.9	36.8
6FDA-ODA	0.22	0.23	46.1	45.6
6FDA-8ODA-2DAPy	0.37	0.38	55.6	55.4
6FDA-8ODA-2DABA	0.35	0.40	53.6	53.2
6FDA-8ODA-2DBSA	0.37	0.42	40.9	39.9
6FDA-MDA	0.27	0.30	39.8	40.7
6FDA-8MDA-2DAPy	0.34	0.38	44.1	45.3

TABLE VI
Moiety Contributions to Concentration Coefficients and Permeation Activation Energies for Total Flux and Water Flux

	n		E_p (kJ mol^{-1})	
Monomer moieties	Total flux	Water flux	Total flux	Water flux
ODA	0.03	0.03	7.1	6.8
MDA	0.07	0.09	6.3	7.0
DAPy	0.18	0.17	27.0	28.9
DABA	0.41	0.32	51.6	50.7
DBSA	0.37	0.37	0.7	−0.1
6FDA	0.25	0.27	35.6	35.6
BPADA[a]	0.30	0.29	35.0	34.9

[a] Calculated with moiety contribution factors from 6FDA-based membranes.

values of BPADA-based and 6FDA-based polyimide membranes?

In gas separation, group contribution methods for prediction of gas permeability were developed.[28,31] Ideas were borrowed from these methods, and a linear contribution method was proposed.[32] Based on the n values of 6FDA-based polyimide membranes, moiety contribution factors for ODA, MDA, DBSA, DABA, DAPy, and 6FDA were successfully obtained from least squares regression, as shown in Table VI.[32] By applying these moiety contribution factors to BPADA-based membranes, the average values of contribution factors of the BPADA moiety were found to be 0.30 (for total flux) and 0.29 (for water flux). The n values of BPADA-8ODA-2DAPy are predicted to be 0.36 (for total flux) and 0.35 (for water flux), respectively.

In eq. (9), $x_w < 1$, so a larger n value means a smaller increase in permeation flux. For total flux, n values of the moieties are in the following order: DABA > DBSA > BPADA > 6FDA > DAPy > MDA > ODA. Moieties with positive effects on the permeation of penetrants cause higher flux even with a lower water content in the feed, so the lower increasing rates of flux are reasonable. Side group effects (including steric and hydrophilic effects) of DABA and DBSA are beneficial to the permeation of water, and the hydrophilicity of imide rings give BPADA and 6FDA the larger n values. The validity of the calculated n values of the BPADA moiety is confirmed from the comparison with those of 6FDA. Since the BPADA moiety is more hydrophilic and more flexible than 6FDA, the larger n values are reasonable. Compared with MDA and ODA, DAPy increases the distribution concentration of the imide rings of BPADA and 6FDA, and as a result DAPy has larger n values. The MDA moiety is more favorable to the permeation of penetrants than the ODA moiety, so the lower increase rate can be found. Interestingly, the n values DABA > DBSA for total flux, while for water flux DABA < DBSA, which indicates the greater steric effect of DABA, the greater hydrophilicity of DBSA.

Effects of the operating temperature

Pervaporation was performed with aqueous isopropanol solutions (~ 20 wt % water), and operating temperatures were controlled at 30–70°C. Figure 7 shows total flux and the permeate water contents. Consistent with the behaviors in the study of the effects of feed concentrations, membranes containing MDA moieties show lower water contents in permeates. Higher permeate water contents are produced by BPADA-MDA membrane, indicating a favorable effect on the permeation of water from the thermal movement of MDA moieties. The permeation of isopropanol is also enhanced in BPADA-ODA membrane, which may result from the higher sorption of isopropanol at elevated temperatures.

The effects of temperature on pervaporation properties are much more complicated than the effects of the feed concentrations. At a higher operating temperature, the diffusion of penetrants is definitely improved with the higher mobility of polymer segmental chains, but at the same time, the sorption of

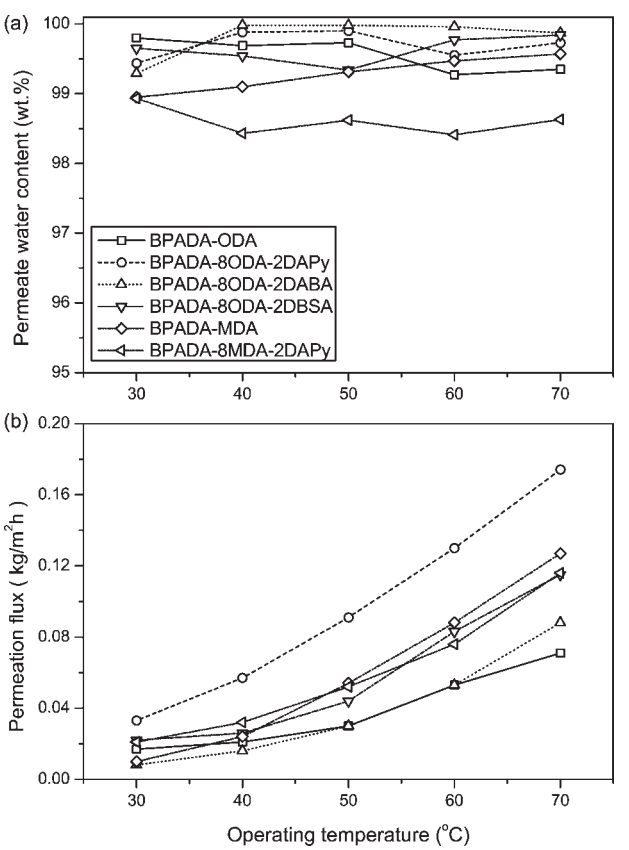

Figure 7 Total flux and permeate water contents for pervaporation with feed water contents of ~ 20 wt %.

penetrants is also greatly affected. In some cases, sorption properties are crucial to determine membrane selectivities.

Permeation activation energies can be decided using the Arrhenius equation. Similar to the concentration coefficients proposed, permeation activation energies tell the increasing rate of the flux when increasing the operating temperature. Activation energies for total flux and water flux were calculated and are listed in Table V, together with the activation energies of 6FDA-based membranes, for the purpose of comparison. However, no distinct difference can be told between 6FDA-based membranes and BPADA-based membranes.

The linear moiety contribution method was also applied to the activation energies, and the least squares regression was made using activation energies of 6FDA-based membranes. The moiety contribution factors were obtained for ODA, MDA, DBSA, DABA, DAPy, and 6FDA moieties from the regression, and the contributions of BPADA moiety to the activation energies were calculated by deduction of the contributions of the other moieties from BPADA-based membranes. Average values of the contributions of BPADA were decided to be 35.0 $kJ\,mol^{-1}$ (for total flux) and 34.9 $kJ\,mol^{-1}$ (for water flux in permeates). Differences between the activation energies for total flux and those for water flux are not significant.

The largest contribution to the activation energies is made by DABA moieties, possibly because large transient gaps favorable to the diffusion of water are produced at a higher temperature. Diffusion-related properties, including side group effects, distribution concentration effects, and the flexibility of the polymer chains, are dominant in the contributions to activation energies, and an order can be observed: DABA > 6FDA and BPADA > DAPy > ODA and MDA. The DBSA moiety with a larger side group, however, has the smallest contribution, probably due to the lower sorption of water at higher temperatures, and the strong interaction between water and the sulfonic acid group is thermally sensitive, yielding the negative contribution to the activation energy for water flux.

CONCLUSIONS

Six polyimides with high molecular weights were successfully synthesized from BPADA and various diamines and were characterized with GPC, DSC, FTIR, NMR, DSC, and TGA.

DSC results showed that the contributions from the diamines to the glass transition temperatures were in an order: DAPy > DABA > DBSA > ODA. Polyimides showed good thermal stabilities, and the apparent activation energies for thermal decomposition were calculated.

Polyimide membranes were prepared from the THF solutions, and their hydrophilicity was estimated by contact angles and the water-membrane interfacial free energies. BPADA-MDA was more hydrophilic than the others.

Pervaporation properties were investigated for dehydration of isopropanol, and comparisons were made between BPADA-based membranes and 6FDA-based membranes. The *concentration coefficients* of BPADA-based membranes were calculated from the linear moiety contribution method. Temperature effects on permeation flux were studied with permeation activation energies for total flux and water flux in permeates. The linear moiety contribution method was applied to the *concentration coefficients* and activation energies. The contribution factors of the BPADA moiety for the *concentration coefficients* are found to be 0.30 (for total flux) and 0.29 (for water flux), respectively. The *concentration coefficients* of BPADA-8ODA-2DAPy are amended to be 0.36 (for total flux) and 0.35 (for water flux), respectively. The contribution factors of the BPADA moiety for activation energies were determined to be 35.0 kJ/mol (for total flux) and 34.9 kJ/mol (for water flux in permeates). It is revealed that the steric effects of the monomers may change the diffusion properties, while functional groups are probably favorable to the changes in sorption properties.

References

1. Huang, R. Y. M., Ed. Pervaporation Membrane Separation Processes; Elsevier: Amsterdam, 1990.
2. Sullivan D. M.; Bruening, M. L. J Membr Sci 2005, 248, 161.
3. Xiao, S.; Huang, R. Y. M.; Feng, X. J Membr Sci 2006, 286, 245.
4. Adrova, N. A.; Bessonov, M. I.; Laius, L. A.; Rudakov, A. P., Eds. In Polyimides, A New Class of Thermally Stable Polymers; Schiller, A. M., Ed.; Thechnomic Publishing: Stamford, 1970.
5. Bessonov, M. I.; Konton, M. M.; Kudryavtsev, V. V.; Laius, L. A. Polyimides, Thermally Stable Polymers; Consultants Bureau: New York, 1987.
6. Sroog, C. E. Prog Polym Sci 1991, 16, 561.
7. Huang, R. Y. M.; Feng, X. Sep Sci Technol 1992, 27, 1583.
8. Huang, R. Y. M.; Feng, X. Sep Sci Technol 1993, 28, 2035.
9. Huang, R. Y. M.; Feng, X. J Membr Sci 1993, 84, 15.
10. Feng, X.; Huang, R. Y. M. J Membr Sci 1996, 109, 165.
11. Yanagishita, H.; Maejima, C.; Kitamoto D.; Nakane, T. J Membr Sci 1994, 86, 231.
12. Qiao, X.; Chung, T.-S.; Pramoda K. P. J Membr Sci 2005, 264, 176.
13. Qiao, X.; Chung, T.-S. Ind Eng Chem Res 2005, 44, 8938.
14. Liu, R.; Qiao, X.; Chung, T.-S. Chem Eng Sci 2005, 60, 6674.
15. Guo, W. F.; Chung, T.-S. J Membr Sci 2005, 253, 13.
16. Zhou, F.; Koros, W. J Polymer 2006, 47, 280.
17. Qariouh, H.; Schue, R.; Schue, F.; Bailly, C. Polym Int 1999, 48, 171.
18. Kaba, M.; Raklaoui, N.; Guimon, M.-F.; Mas, A. J Appl Polym Sci 2005, 97, 2088.

19. Qiao, X.; Chung, T.-S. AICHE J 2006, 52, 3462.
20. Li, C.-L.; Lee, K.-R. Polym Int 2006, 55, 505.
21. Teng, M.-Y.; Li, C.-L.; Lee, K.-R.; Lai, J.-Y. Desalination 2006, 193, 144.
22. Xu, Y.; Chen, C.; Zhang, P.; Sun, B.; Li, J. J Chem Eng Data 2006, 51, 1841.
23. Xu, Y.; Chen, C.; Li, J. Chem Eng Sci 2007, 62, 2466.
24. Wang, L.; Li, J.; Zhao, Z.; Chen, C. J Macromol Sci Pure Appl Chem 2006, 43, 305.
25. Wang, Y. C.; Tsai, Y. S.; Lee, K. R.; Lai, J. Y. J Appl Polym Sci 2005, 96, 2046.
26. Kang, Y. S.; Jung, B.; Kim, U. Y. Mol Cryst Liq Cryst 1993, 224, 137.
27. Okamoto, K.; Tanihara, N.; Watanabe, H.; Tanaka, K.; Kita, H.; Nakamura, A.; Kusuki, Y.; Nakagawa, K. J Membr Sci 1992, 68, 53.
28. Salame, M. Polym Eng Sci 1986, 26, 1543.
29. Jia, L.; Xu J. Polym J 1991, 23, 1.
30. Park, J. Y.; Paul, D. R. J Membr Sci 1997, 125, 23.
31. Robeson, L. M.; Smith, C. D.; Langsam, M. J Membr Sci 1997, 132, 33.
32. Xiao, S.; Huang, R. Y. M.; Feng, X. Polymer 2007, 48, 5355.
33. Silverstein, R. M.; Bassler, G. C.; Morrill, T. C. Spectrometric Identification of Organic Compounds; Wiley-Interscience: New York, 1997.
34. Dunson, D. L. Synthesis and Characterization of Thermosetting Polyimide Oligomers for Microelectronics Packaging; PhD dissertation, Virginia Tech, 2000.
35. Pramoda, K.; Liu, S.; Chung, T.-S. Macromol Mater Eng 2002, 287, 931.
36. Sroog, C. E.; Endrey, A. L.; Abramo, S. V.; Berr, C. E.; Edwards, W. M.; Olivier, K. L. J Polym Sci Part A 1965, 3, 1373.
37. Nakanishi, K.; Solomon, P. H. Infrared Absorption Spectroscopy, 2nd ed.; Holden-Day: San Francisco, 1977.
38. Li, Y.; Wang, X.; Ding, M.; Xu, J. J Appl Polym Sci 1996, 61, 741.
39. Broido, A. J Polym Sci Part A-2: Polym Phys 1969, 7, 1761.
40. Schrader, M. E.; Loeb, G., Eds. Modern Approach to Wettability: Theory and Applications; Plenum Press: New York, 1991.
41. Oh, E.; Luner, P. E. Int J Pharm 1999, 188, 203.
42. De Bartolo, L.; Gugliuzza, A.; Morrelli, S.; Cirillo, B.; Gordano, A.; Drioli, E. J Mater Sci: Mater Med 2004, 15, 877.
43. Van Oss, C. J.; Giese, R. F.; Wu, W. J Adhesion 1997, 63, 71.
44. Du, R.; Chakma, A.; Feng, X. J Membr Sci 2007, 290, 19.
45. Van Oss, C. J.; Giese, R. F. Clays Clay Miner 1995, 43, 474.
46. Koros, W. J.; Fleming, G. K. J Membr Sci 1993, 83, 1.
47. Kuznicki, S. M.; Langner, T. W.; Curran, J. S.; Bell, V. A. US Patent 6379436 (2002).
48. Perry, J. D.; Nagai, K.; Koros, W. J MRS Bull 2006, 31, 745.
49. Comyn, J., Ed. Polymer permeability; Elsevier Applied Science Publishers: London and New York, 1986.